NJC

PAPER

View Article Online
View Journal | View Issue

Published on 21 July 2015. Downloaded by University of Zululand on 06/10/2015 13:12:41.

Cite this: *New J. Chem.*, 2015, 39, 7251

CdSe quantum dots capped with naturally occurring biobased oils†

Joseph W. Kyobe,[abc] Egid B. Mubofu,[a] Yahya M. M. Makame,[a] Sixberth Mlowe[b] and Neerish Revaprasadu*[b]

Received (in Nottingham, UK) 9th June 2015,
Accepted 8th July 2015

DOI: 10.1039/c5nj01460c

www.rsc.org/njc

We report a green synthesis of CdSe quantum dots (QDs) using bio-based materials (castor oil and ricinoleic acid) as capping agents. The absorption spectra of the as-synthesized CdSe QDs showed typical features of quantum confinement. The particle sizes of QDs were determined using the absorption band edges and found to be 3.81 to 6.80 nm and 5.91 to 8.31 nm for the entire range of reaction temperatures for QD-capped with castor oil (CSTO) and ricinoleic acid (RA), respectively. The photoluminescence spectra showed narrow emission peaks. The transmission electron microscopy (TEM) images showed spherical particles with sizes comparable to those determined from the absorption spectra. Comparatively, large particles were observed for RA capped CdSe QDs than those stabilized by CSTO. X-ray diffraction patterns revealed that the synthesized CdSe quantum dots have cubic structure. The particle sizes of CdSe deduced from X-ray diffraction measurements were in excellent agreement with those deduced from absorption spectra and TEM images. The *d*-spacings from the HRTEM images were consistent with those reported in literature. The surface area and the agglomeration number for as-synthesized CdSe QDs of different sizes are also reported.

Introduction

The rate of chemical synthesis of nanoparticles or quantum dots has increased exponentially over the last few decades. Amongst the compound semiconductor materials, CdSe with its tunable band gap and bright emission was identified as a 'cinderella' material with properties suitable for a wide range of applications. Its use in light emitting diode devices,[1–3] solar cells,[4–6] fluorescent probes in biology[7–10] and aerospace applications[11] has been well documented. CdSe nanoparticles have intense luminescence and photo-stability making them good candidates for biosensor lasers.[12] Consequently CdSe became one of the most studied semiconductor materials. However recent interest in CdSe has dwindled due to issues of toxicity. The behaviour and toxicity inference of nanoparticles mainly comes from studies on inhaled nanoparticles.[13]

The early work on CdSe synthesis was dominated by studies done by Bawendi and Alivisatos groups.[14–19] Later, Peng and others reported environmentally friendly routes to CdSe which subsequently led to many other environmentally benign synthetic methodologies.[20–22] The "green" synthesis of nanostructured materials is still an emerging area within the realm of nanoscience. Most of the green protocols involve the replacement of toxic capping agents and solvents with non-toxic naturally occurring materials. For instance, anacardic acid,[23] tartaric acid/triethanolamine,[24,25] olive oil[26,27] and glycerol/oleic acid[28] have been used as green solvents and capping agents in synthetic routes to stabilize CdSe nanocrystals. Therefore the green protocols for the fabrication of CdSe QDs (nanocrystals) using naturally occurring bio-based substances as solvents and capping agents can be considered as a very promising and attractive area in nanotechnology.

Castor oil is an environmentally renewable raw material[29] that contains no toxic protein residuals.[30] It is non-edible oil and is a mixture of triglyceride with a combination of saturated and unsaturated fatty acids attached to glycerol (Fig. 1). The oil comprises a high percentage of ricinoleic acid (12-hydroxyl-*cis*-octadec-9-enoic acid)[31] and its structural features[32] are capable of forming non-covalent bonds (coordination interactions) or acid/base interaction between the oxygen atoms (O^{2-}) of the ligands with active surface dangling orbitals of CdSe quantum dots. In this study, we report a green synthesis of CdSe quantum dots using castor oil and ricinoleic acid as eco-friendly bio-based capping agents. In addition, the use of castor oil and ricinoleic acid as both capping and dispersing agents eliminates the need

[a] *Department of Chemistry, University of Dar es Salaam, P.O. Box 35061, Dar es Salaam, Tanzania*
[b] *Department of Chemistry, University of Zululand, Private Bag X1001, Kwa-Dlangezwa, 3886, South Africa. E-mail: RevaprasaduN@unizulu.ac.za; Fax: +27 35 902 6568; Tel: +27 35 902 6152*
[c] *Department of Chemistry, St. John's University of Tanzania, P.O. Box 47, Dodoma, Tanzania*

† Electronic supplementary information (ESI) available. See DOI: 10.1039/c5nj01460c

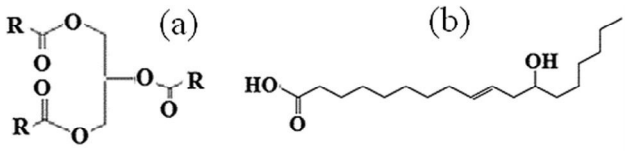


Fig. 1 General structure of (a) castor oil and (b) ricinoleic acid.

Published on 21 July 2015. Downloaded by University of Zululand on 06/10/2015 13:12:41.

for the use of air-sensitive, toxic and expensive chemicals such as TOP, TOPO and alkyl amines. The boiling points of castor oil and ricinoleic acid are 313 and 412 °C, respectively and they are simple to work with since they are liquid at room temperature. The objective is to use a green synthetic protocol to prepare monodispersed and high quality CdSe quantum dots and to investigate the effect of quantum confinement on their optical properties. The particle size, structure and morphology of the prepared CdSe quantum dots will be discussed.

Results and discussion

Optical properties of CdSe nanoparticles

CdSe quantum dots were synthesized by the reduction-thermolysis route, using castor oil and ricinoleic acid as capping agents. The effects of the capping agents, time and thermolysis temperature on the CdSe QDs were investigated using the absorption spectroscopic technique. The spectra were collected using acetone as a dispersing solvent at room temperature. Fig. 2 presents the absorption spectra of CdSe QDs capped with castor oil (Fig. 2a–c) and ricinoleic acid (Fig. 2d–f). Reduction in the quantum confinement displayed in the absorption spectra can be caused by several factors, including increased electronic coupling between QDs and/or particle grain growth. The maximum blue shifted peak (excitonic features) in absorption as compared to bulk CdSe and the corresponding shifted bulk band edges are given in Table 1.

The particle sizes of CdSe QDs were calculated by fitting the absorption maximum wavelengths in Table 1 to the formula described by Peng and his co-workers given in eqn (1).[33] The equation was established using the known CdSe particle sizes measured from TEM images. Other optical properties were obtained by utilizing the direct band method.[34]

$$S = (1.6122 \times 10^{-9})\lambda^4 - (2.6575 \times 10^{-6})\lambda^3 + (1.6242 \times 10^{-3})\lambda^2 - (0.4277\lambda + 41.57) \quad (1)$$

where S (nm) is the size of a given CdSe QD sample (nm) and λ (nm) is the wavelength of the first optical excitonic peak of the corresponding sample also in nanometres. Within this work, we have made comparisons with the size dependent extinction coefficient equation proposed by Mulvaney *et al.*[35] We found that the CdSe QDs with first exciton absorption peaks listed in Table 1 obey the equation giving CdSe QD diameters (S) between 3.94–6.10 nm and 5.90–7.80 nm for CSTO and RA capped CdSe QDs, respectively. These nanocrystal diameters (S) are in excellent agreement with those determined by Mulvaney and co-workers[35] between 2 and 8 nm within the same range of reaction temperatures with different capping agents. Nevertheless, swapping out solvent for another or capping agent for another is not a necessity for similar results.

These results (Table 1 and Fig. 2) clearly show that when the reaction time was prolonged there was a change in the size and optical properties of the CdSe QDs. The red-shift expected through a change in the first absorbance maximum wavelength as a function of time or temperature is evident. The results also show that the size distribution of CdSe QDs is narrower for a short growth time. Temperature can also be used to control the average size of the CdSe QDs. For example, the particle size of CdSe QDs synthesized at 230 °C for 30 minutes is smaller than those prepared at 280 °C for the same period of time and reaction conditions. The capping layer of castor oil (CSTO) molecules is strongly coordinated to the surface dangling orbital of CdSe compared to that of the ricinoleic acid (RA) molecules.

This is possibly associated with the availability of the ester linkage and the three hydroxyl groups in CSTO as opposed to a single hydroxyl group in the 12-carbon and the carboxylic group in RA. Even though the carboxylic acid end group of RA is a useful conjugation site, the other hydroxyl group on 12-carbon is less reactive and is not readily available for non-covalent attachment to CdSe sites. Essentially, the driving force behind the nature of capping agents is the high affinity of castor oil (CSTO) towards the surfaces of CdSe QDs slowing down the rate of aggregation and precipitation of CdSe QDs.

Fig. 3 shows the typical features of regression lines for particle size growth as a function of time for isothermal synthesis of CdSe QDs at various preparation temperatures. The slopes of the lines are indicative of the rate of growth of CdSe quantum dots and hence justifies that the growth of particle sizes is linear (simple first order reaction mechanism) with good correlation coefficients close to 1. The particle size increase during aging for CSTO-CdSe (Fig. 3a) and RA-CdSe QDs (Fig. 3b) shows that castor oil coordinates to CdSe surfaces stronger than ricinoleic acid and hence prevents the particle growth stronger than ricinoleic acid.

The correlation between quantum dot sizes and their optical electronic behaviour is very important for exploring the novel properties of nanocrystalline systems. The absorption spectra of CdSe QDs at room temperature (Fig. 2) show excitonic absorption peaks and the corresponding shifted band edges. There is a clear blue shift of band gaps with respect to bulk CdSe. This is due to the modification of valence and conduction bands by quantum confinement effects.[36,37] For small nanocrystals (*i.e.* strong confinement regime) the electron and hole can be treated as independent and the optical spectra can be viewed as transitions between the electron (e) and hole (h) quantised levels. Thus the band gap state in this confinement regime is the effective mass approximation method (EMA) given in eqn (2).[36]

$$\Delta E = \frac{h^2}{8S^2\mu} - \frac{1.8e^2}{\varepsilon_{CdSe}4\pi\varepsilon_o S} \quad (2)$$

where ΔE is the band gap energy difference between the semiconductor CdSe QD and the bulk CdSe semiconductor, h is

 This journal is © The Royal Society of Chemistry and the Centre National de la Recherche Scientifique 2015

Published on 21 July 2015. Downloaded by University of Zululand on 06/10/2015 13:12:41.

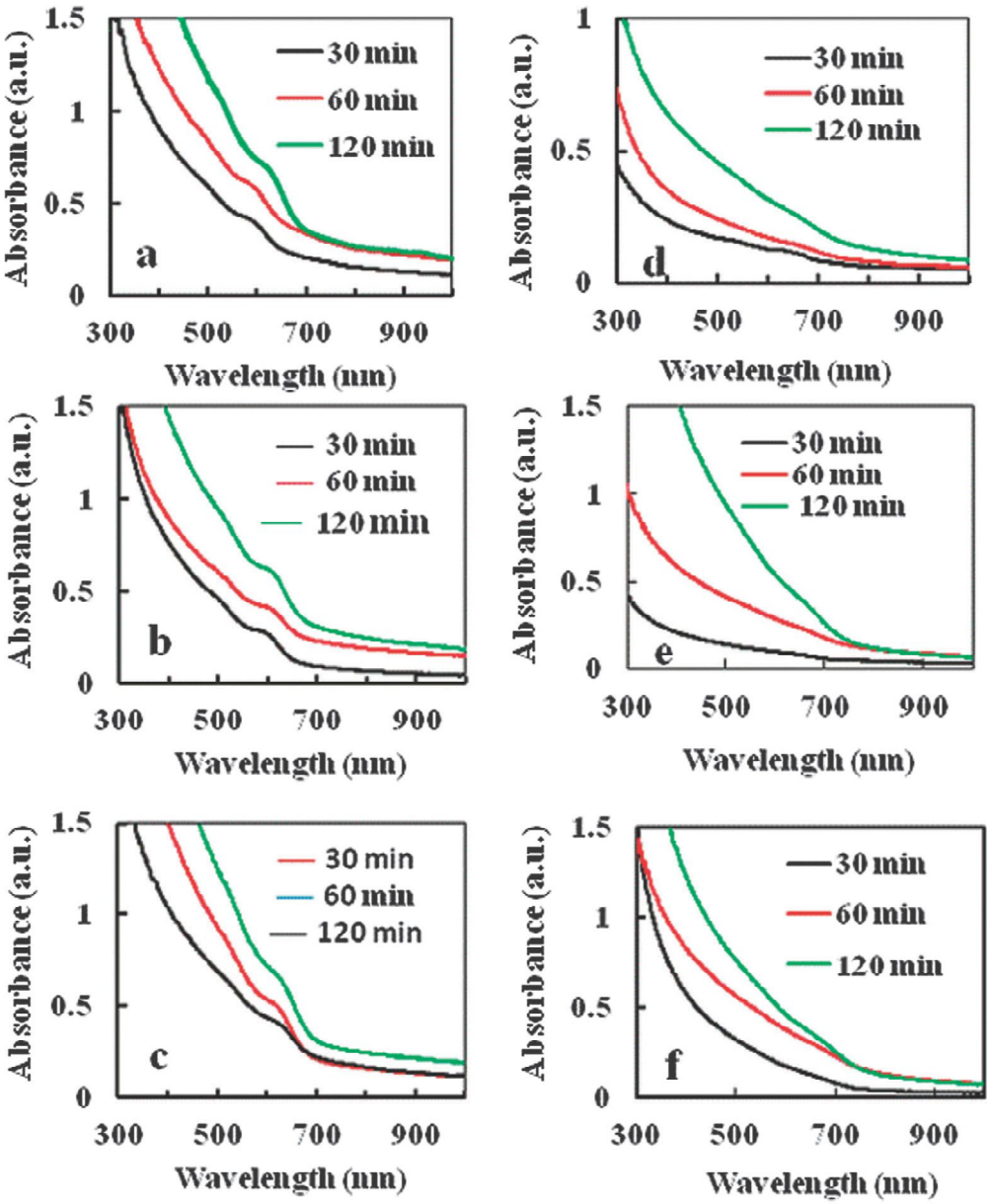


Fig. 2 Absorption spectra of (a–c) castor oil and (d–f) ricinoleic acid capped CdSe nanocrystals. The thermolysis reactions were carried out at 230 °C (a and d), 250 °C (b and e) and 280 °C (c and f).

Planck's constant, S is the particle size, e is the electronic charge, ε_{CdSe} is the dielectric constant, ε_o is the permittivity of free space and $\mu = m_e^* m_h^*/(m_e^* + m_h^*)$ is the reduced mass where m_e^* and m_h^* are the effective masses of the excited electron and the electron hole. For CdSe nanocrystals, $m_e^* = 0.13m_o$, $m_h^* = 0.45m_e$ (m_e is the rest mass of an electron) and $\varepsilon_{CdSe} = 10.2$.[38] Using these values, eqn (2) is modified to eqn (3), where the energy values are in eV and S in nm.

$$\Delta E = \frac{3.723}{S^2} - \frac{0.254}{S} \quad (3)$$

Introducing the CdSe QD first absorption peaks and band edges in either eqn (2) or (3), we calculated the CdSe QD sizes and they are given in the ESI,† Table S1. We have also fitted the experimental CdSe QD data to a simple exponential function proposed by Bacherikov and his co-workers[39] in calculating the size of the CdSe QDs (eqn (4)).

$$S = 0.344 \exp\left(\frac{\lambda_{max} - 252.7}{129.3}\right) \quad (4)$$

where S is the average particle size in nm. This equation is applicable for nanocrystals falling within the quantum size effect ranging up to 10 nm. Introducing the values of first UV-vis excitonic peak position wavelengths in eqn (4), we calculated the CdSe crystalline sizes as reported in the ESI,† Table S1. The resulting average crystal size of CdSe particles compares favourably with those determined from eqn (1) and (2) with reasonable limits of errors.

Published on 21 July 2015. Downloaded by University of Zululand on 06/10/2015 13:12:41.

Table 1 Optical parameters and size of CdSe quantum dots obtained from the UV-vis absorption spectra at room temperature and eqn (1), respectively

T (°C)	t (min)	Absorption peak λ_{max} (nm)	Shifted band edge λ_{BE} (nm)	Particle size S (nm) eqn (1)
Castor oil-capped CdSe QDs				
230	30	580	645	3.82
	60	585	650	3.99
	120	595	665	4.37
250	30	590	650	4.17
	60	595	660	4.37
	120	610	675	5.06
280	30	610	680	5.06
	60	620	690	5.61
	120	630	695	6.23
Ricinoleic acid-capped CdSe QDs				
230	30	625	690	5.91
	60	630	730	6.23
	120	640	740	6.95
250	30	635	695	6.58
	60	640	735	6.95
	120	650	745	7.76
280	30	640	735	6.95
	60	645	755	7.34
	120	655	755	8.31

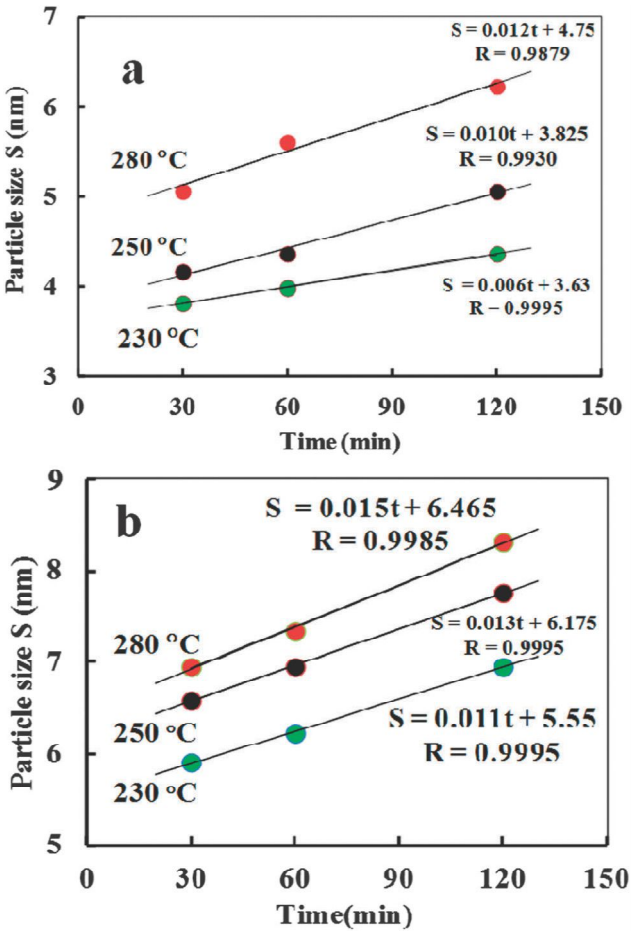


Fig. 3 Regression lines for particle size growth as a function of refluxing time for isothermal synthesis of CdSe capped with (a) castor oil and (b) ricinoleic acid at various temperatures.

The CdSe QD sizes calculated based on the EMA (eqn (2)) model using absorbance onset wavelengths do not match with those calculated from eqn (1) and (3) (ESI,† Table S1). However, the model gives comparable CdSe QD sizes when shifted bulk band edge wavelengths (λ_{BE}) were used in the calculations. This discrepancy arises because the EMA model breaks down in small QD regimes since the energy–wave vector (E–k) relationship can no longer be approximated as parabolic.

The approximations made in reaching the EMA model are not valid for small particles due to deviations in the estimated values such as electron–hole effective masses which are applicable for bulk substances. However, the optical shifted band edges of the RA capped CdSe at higher temperatures with prolonged reaction grow exceedingly the bulk band gap energy of CdSe (712.6 nm). Under these circumstances, the EMA method (eqn (2)) was unable to accommodate such effects (ESI,† Table S1) which account for the disagreement with eqn (1) and (4) at higher temperatures. The shifted band edge in this case moves towards the red end of the visible spectrum. The average sizes of as-synthesized CSTO/RA capped-CdSe QDs obtained from eqn (1), (2) and (4) for each reaction temperature are given in the ESI,† Table S1.

The CdSe QD formation takes place due to agglomeration of a single particle (primary particle). The agglomeration number (*i.e.* the extinction coefficient per mole) specifies the number of primary particles or molecules contained in a single CdSe QD at a given size.[40] This number is strongly dependent on the size of the CdSe QD and is independent of the capping agent on the QD surface, solvent used to dissolute the particles and temperature. Assuming the spherical geometry of the CdSe QD, its surface area is given by eqn (5).

$$a = Bm^{2/3} \quad (5)$$

where a and m are the surface area and the mass of CdSe quantum dots respectively, $B = (36\pi/\rho^2)^{1/3}$ is a constant and ρ is the density of CdSe (5.82 g cm^{-3}). Table 2 presents the values of the surface area (a), mass (m) and number of particles (agglomeration number) for the as-synthesized castor oil/ricinoleic acid capped CdSe quantum dot calculated on the basis of the particle size listed in the ESI,† Table S1. The molar mass of CdSe = 191.36 g per mole and Avogadro's number (N_A) = 6.023 × 10^{23} atoms were used to calculate the number of atoms in a single quantum dot and are included in Table 2.

Plotting the graphs of the surface area or agglomeration number (Table 2) against the particle size, smooth curves are obtained (Fig. 4). This shows that the agglomeration number (n) of nearly mono-dispersed CdSe quantum dots increases as a cubic function in a quantum confinement regime given by:

$$n = Ar^3 \quad (6)$$

where $r(S/2)$ is the radius in nanometers, $A = 4\pi N_A/3V_m$ is a constant and V_m is the molar volume of CdSe. Both eqn (5) and (6) give a plausible explanation on how the decrease of particle size leads to a very large surface to volume ratio for nanocrystals.

The photoluminescence emission spectra of the prepared CdSe quantum dots capped with castor oil and ricinoleic acid

 This journal is © The Royal Society of Chemistry and the Centre National de la Recherche Scientifique 2015

Published on 21 July 2015. Downloaded by University of Zululand on 06/10/2015 13:12:41.

Table 2 Values of surface area (*a*), mass (*m*) and number of particles/agglomeration number (*n*) in a single CdSe quantum dot calculated for different sizes of as-synthesized CdSe quantum dots using eqn (5)

Particle size *S* (nm)	Surface area *a* (nm^2)	Mass of CdSe QD $m \times 10^{-22}$ kg	Number of particles (*n*)
Castor oil stabilized CdSe QDs			
3.82	45.8434	1.6987	535
3.99	50.0145	1.9357	609
4.17	54.6288	2.2097	695
4.37	58.9947	2.5431	800
5.06	80.4361	3.9480	1243
5.61	98.8725	5.3804	1693
6.23	121.9343	7.3681	2319
Ricinoleic acid stabilized CdSe QDs			
5.91	109.7299	6.2905	1980
6.23	121.9343	7.3686	2320
6.58	136.0197	8.6816	2730
6.95	151.7468	10.2300	3220
7.34	169.2552	12.0506	3790
7.76	189.1792	14.2399	4480
8.31	216.9462	17.4874	5500

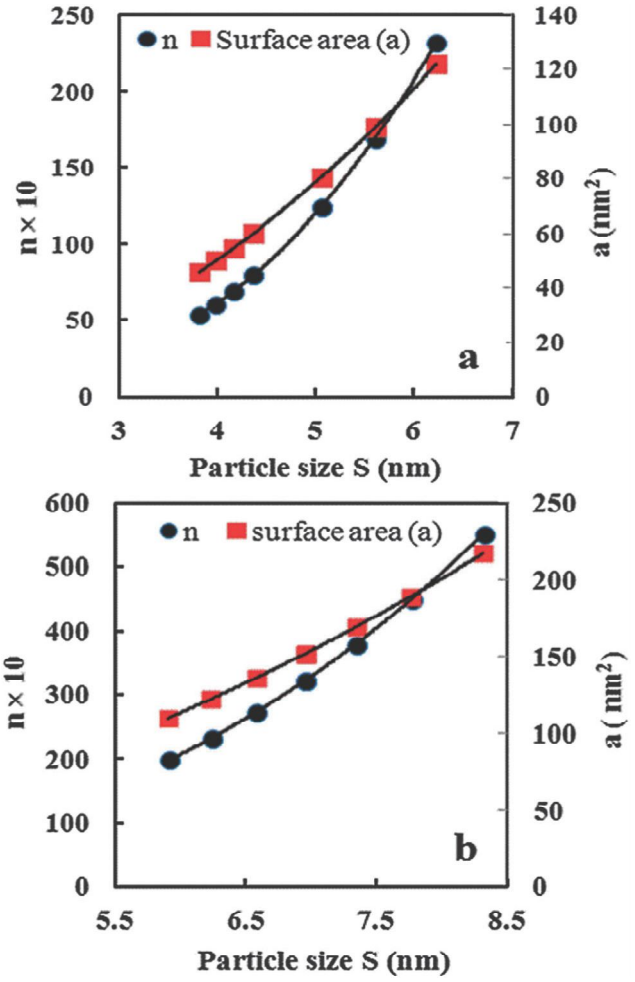


Fig. 4 Plots of agglomeration number (*n*) and surface area against the particle size of as-synthesized (a) castor oil and (b) ricinoleic acid capped-CdSe quantum dots.

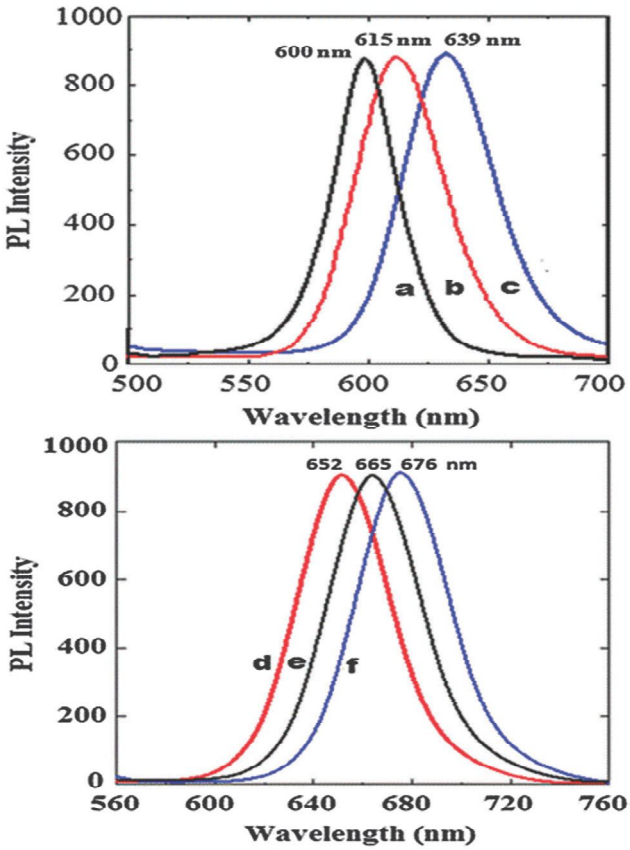


Fig. 5 Photoluminescence spectra of CdSe quantum dots as-synthesized in castor oil (a–c) and ricinoleic acid (d–f) at 230 °C, 250 °C and 280 °C for 30 minutes.

are shown in Fig. 5 at an excitation wavelength of 400 nm. All samples showed well defined, narrow emission peaks centred at 600, 615, and 639 nm (Fig. 5a–c) and 652, 665 and 676 nm (Fig. 5d–f) for castor oil and ricinoleic acid stabilized CdSe quantum dots, respectively. The photoluminescence emission peaks occur at lower energies than absorption maxima which indicates that molecules bearing excited electrons have weaker bonds than those with electrons at the ground state. Effective Stoke shifts ranged from 25 to 30 nm and 27 to 36 nm for castor oil and ricinoleic acid capped CdSe QDs, respectively. The full width at half maximum (FWHM) of castor oil and ricinoleic acid capped CdSe was measured and found to be in the range of 28–50 nm. The locus of peaks towards the red end of the visible spectrum (red shift) occurs with the growth time and/or temperature. This is consistent with the particle in a box theory where longer time corresponds to larger crystals, lower energy electronic emission and thus longer wavelengths.[41] We observe the variation in the absorption peak position with temperature similar to that of photoluminescence showing that the optical transition for both photoluminescence and absorption is similar in nature.

Morphological studies

The TEM and HRTEM images of CdSe QDs capped with castor oil synthesized at 280 °C are shown in Fig. 6. From the TEM

Published on 21 July 2015. Downloaded by University of Zululand on 06/10/2015 13:12:41.

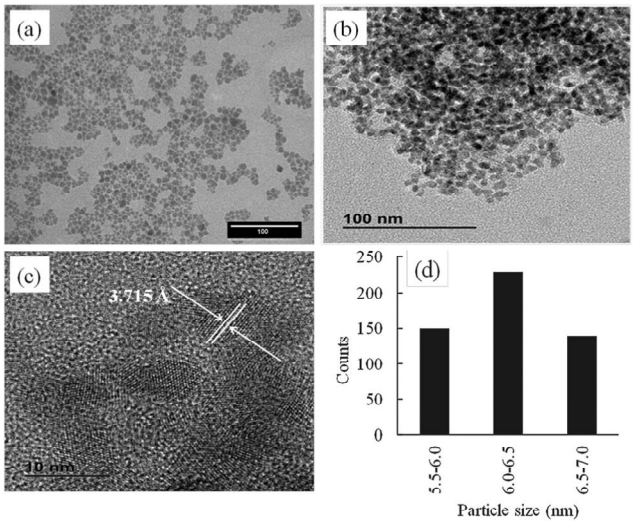


Fig. 6 TEM images (a and b), HRTEM image (c) and particle size histogram (d) of castor oil capped CdSe quantum dots synthesized at 280 °C for 2 hours.

images (Fig. 6a and b), the prepared CdSe QDs are monodispersed with nearly spherical shapes with an average particle size of 6.11 ± 0.01 nm (Fig. 6d). This value of CdSe QD particle size deduced from TEM images compares well with those determined from absorption spectra using eqn (1)–(3). The HRTEM images in Fig. 6c show particles with distinct lattice fringes appearing in one or more directions, surrounded by the capping matrix. An average *d*-spacing of 3.715 ± 0.013 Å is indexed to the (111) reflection planes, consistent with the standard *d*-spacing of a cubic CdSe (card number: 019-0191). The fringes in HRTEM images are the projection of tunnels between columns of atoms and the dark lines are the atoms themselves.

In comparison to CSTO-capped CdSe QDs, larger particle sizes were observed for the RA capped CdSe QDs (Fig. 7). This increase in particle size could be associated with the weak passivating capacity of ricinoleic acid to the CdSe surface as discussed earlier. The average particle size of ricinoleic acid capped CdSe QDs deduced from the TEM images was 7.60 ± 0.46 nm (Fig. 7a and b) in good agreement with that determined from the UV-spectra. The representative HRTEM images of RA stabilized CdSe QDs (Fig. 7c and d) reveal clear fringes with a lattice separation of 3.542 Å assigned to the (111) reflection plane of cubic CdSe.

Structural studies

Fig. 8a shows the powder XRD pattern of the castor oil-stabilised CdSe quantum dots synthesized at 230 and 250 °C. The pattern shows the presence of (111), (220) and (311) reflection planes of the cubic phase of CdSe [Card #; 019-0191]. The XRD patterns of the as-synthesized castor oil and ricinoleic

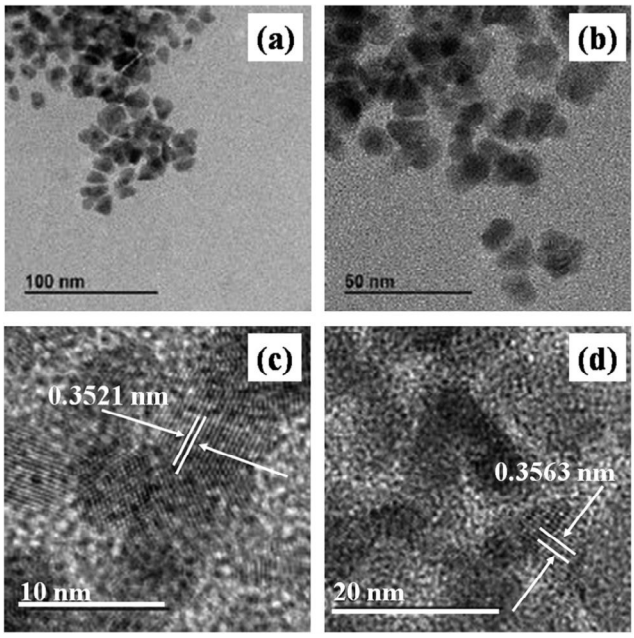


Fig. 7 TEM images (a and b) and HRTEM images (c and d) of ricinoleic acid capped CdSe quantum dots synthesized at 280 °C for 2 hours.

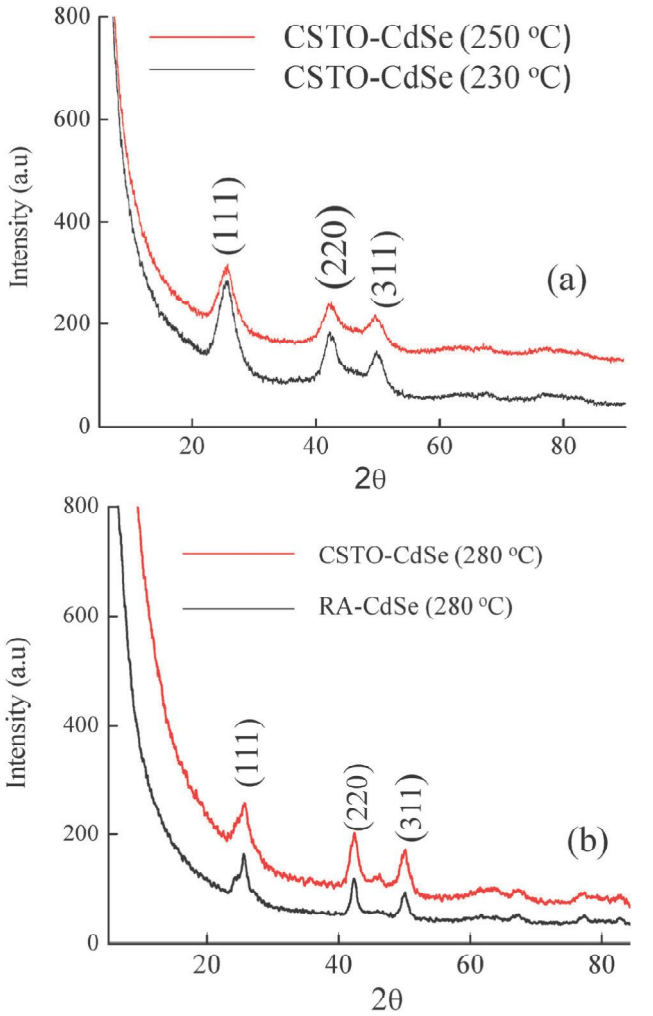


Fig. 8 XRD patterns of (a) CSTO-capped CdSe QDs synthesized at 230 and 250 °C, and (b) RA and CSTO capped CdSe QDs prepared at 280 °C.

 This journal is © The Royal Society of Chemistry and the Centre National de la Recherche Scientifique 2015

Published on 21 July 2015. Downloaded by University of Zululand on 06/10/2015 13:12:41.

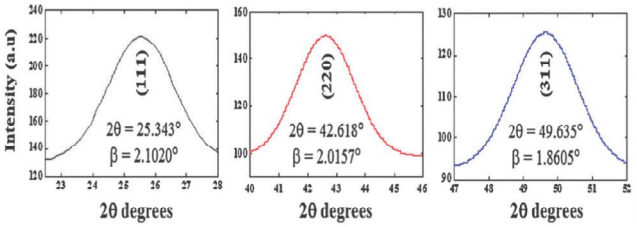


Fig. 9 The fit Gaussian plots at (111), (220) and (311) planes for castor oil capped-CdSe quantum dots prepared at a temperature of 230 °C.

acid-capped CdSe quantum dots at 280 °C are shown in Fig. 8b. The patterns show the presence of (111), (220), (311), (331), (422) and (511) reflection planes assigned to the cubic phase of CdSe. The average crystalline sizes of the CdSe QDs were calculated using Debye–Scherrer's formula[42] and is given by

$$S = \frac{B\lambda}{\beta \cos\theta} \quad (7)$$

where S is the size of CdSe QDs which assumed a spherical shape, B is a coherent constant (0.91), λ is the X-ray wavelength (1.5406 Å), and β is the width of the broadening XRD peaks. For castor oil capped-CdSe quantum dots as-synthesized at 230 °C, the values of β and θ corresponding to the (111), (220) and (311) planes were estimated from the Gaussian plots shown in Fig. 9. Making use of these data, the crystalline sizes of 3.82, 3.99 and 4.34 nm were calculated according to eqn (7). The average crystalline size was found to be 4.10 ± 0.22 nm in good agreement with the size determined by other methods (Table 2 and TEM). From the X-ray diffraction pattern of ricinoleic acid capped-CdSe quantum dots (Fig. 8b), the crystalline particle sizes calculated were 6.67, 8.63 and 7.76 nm corresponding to the (111), (220) and (311) planes, respectively. The mean crystal size of the CdSe particle was 7.69 ± 0.80 nm which corroborates favourably with the size observed from other evaluation methods.

Conclusions

We have used environmentally benign bio-based castor seed extracts as green capping agents in the synthesis of well dispersed CdSe quantum dots. The bio-based chemicals (castor oil and ricinoleic acid) showed excellent capping ability to the synthesis of CdSe quantum dots and afforded monodispersed quantum dots. The extracts are non-edible oils that are readily available, eco-friendly and effective stabilising agents with comparable capping ability to expensive and toxic commercial stabilizing agents. The small sized and nearly spherical CdSe quantum dots ranging between 3.81 and 6.80 nm for castor oil stabilized CdSe quantum dots were achieved whereas ricinoleic acid stabilized CdSe quantum dots were spherical with particle sizes ranging from 5.91 to 8.31 nm. Interestingly, the synthesis process was based on these green oils which performed the role of both dispersing solvent and a capping agent. The UV-visible and photoluminescence of these materials showed that the as-prepared CdSe quantum dots exhibited quantum confinement effects. The electron microscopy (TEM and HRTEM) and X-ray diffraction (XRD) analysis confirms that both castor oil and ricinoleic acid are effective and potential stabilizing materials in producing high quality and monodispersed CdSe quantum dots with castor oil being superior to ricinoleic acid. Castor oil and ricinoleic acid are effective naturally occurring green surfactants for the preparation of very small metal chalcogenide semiconductor nanomaterials.

Experimental details

Materials

Chemicals and reagents used in this study were of analytical grade (over 98%) and were used without further purification. Cadmium chloride salt, acetone and methanol were supplied by Sigma-Aldrich. Sodium borohydride and selenium powder were supplied by Merck and all chemicals were used as received. Castor oil was extracted from castor seeds and its isolate ricinoleic acid from castor oil as per the method described elsewhere.[43] For purity, repeatability and reproducibility, castor oil and its isolate ricinoleic acid were characterized by FTIR and ^{1}H NMR techniques; the results are shown in the ESI.†

Characterisation of CdSe nanoparticles

The CdSe nanocrystals were characterized by UV-vis spectroscopy (Cary 50 spectrophotometer) in the wavelength from 200 to 1000 nm using a quartz cuvette at room temperature. The emission spectra of the CdSe quantum dots were obtained using a Perkin Elmer LS55 luminescence spectrophotometer at room temperature. The CdSe samples for UV-vis and PL measurements were put in quartz cuvettes of 1 cm path length and then analysed. The morphology and the particle size of CdSe samples were characterized by transmission electron microscopy (TEM) using a JEOL 1010 microscope with an accelerating electrical potential of 100 kV. The morphological and structural characteristics of CdSe quantum dots were also obtained using a high resolution transmission electron microscope (HRTEM) coupled with a JEOL 2010 TEM operating at an accelerating electrical potential of 200 kV. The X-ray diffraction was performed using a Bruker AXS D8 diffractometer coupled with CuKα radiation (λ = 1.5406 Å) with target materials at 40 kV, 40 mA in a 2θ range from 0° to 90°. The data collected were used to determine the lattice parameters, the crystallite size and the crystalline phase. Samples for XRD were repetitively washed with excess acetone to ensure a complete removal of excess capping agent, if any and thereafter dried at room temperature.

Reduction of selenium and preparation of CdSe

The method of reducing Se and subsequent preparation of CdSe nanoparticles was adopted using the method reported earlier.[44] Sodium borohydride (0.032 g, 0.8459 mmol) in 20 mL of water and selenium powder (0.0254 g, 0.322 mmol) were mixed in a 25 mL three necked flask where the mixture was magnetically stirred at room temperature under an inert flowing atmosphere for two hours. The reduction of elemental selenium

Published on 21 July 2015. Downloaded by University of Zululand on 06/10/2015 13:12:41.

by sodium borohydride can be summarised in the following stoichiometric reaction.

$$4NaBH_4(aq) + 2Se(s) + 7H_2O \xrightarrow[N_2]{\text{Room temp}} 2NaHSe(aq) + Na_2B_4O_7(aq) + 14H_2(g)$$

Cadmium chloride (0.0648 g, 0.322 mmol) in 20 mL of distilled water was separately added to the almost colourless solution of NaHSe formed and the mixture was magnetically stirred at room temperature for 30 minutes. To a dark red solution formed, excess of methanol was added and within a few minutes bulk colloids of CdSe were precipitated as represented by the following reaction.

$$NaHSe(aq) + CdCl_2(aq) \rightarrow CdSe(aq) + NaCl(aq) + HCl(aq)$$

The solution was centrifuged at 4000 rpm for 5 minutes to collect the bulk CdSe particles.

Preparation of CdSe quantum dots

The bulk CdSe precipitates collected were then dispersed in a coordinating solvent and quickly injected with a syringe into a refluxed 25 mL three necked flask containing hot stirred (6 g) of either castor oil or ricinoleic acid at 230, 250 and 280 °C and the temperatures were isothermally kept for 2 hours. The coordinating solvent used was castor oil or ricinoleic acid. Aliquots were removed at 30, 60 and 120 minute intervals from the reaction mixture into centrifuging test tubes. The samples were then quenched with methanol flocculating CdSe quantum dots and recovered through centrifugation. The recovered CdSe quantum dots were re-dispersed in acetone for characterisation.

Acknowledgements

The authors are grateful to the National Research Foundation (NRF) through the South African Research Chair initiative (SARChi) and the NRF-COSTECH Project for financial support. We thank the Centre for Electron Microscopy, University of Kwa-Zulu Natal for the electron microscopy measurements.

Notes and references

1 J. Zhao, J. A. Bardecker, A. M. Munro, S. M. Liu, Y. Niu, I. K. Ding, J. Luo, B. Chen, A. K. Y. Jen and D. S. Ginder, *Nano Lett.*, 2006, **6**(3), 463.
2 T. E. Rosson, S. M. Claiborne, J. R. McBride, B. S. Stratton and S. J. Rosenthal, *J. Am. Chem. Soc.*, 2012, **134**(19), 8006.
3 R. D. Schaller, N. Sykora, J. M. Pietryga and V. I. Klimov, *Nano Lett.*, 2006, **6**, 424.
4 S. Jiao, Q. Shen, I. Mora-Seró, J. Wang, Z. Pan, K. Zhao, Y. Kuga, X. Zhong and J. Bisquert, *ACS Nano*, 2015, **9**(1), 908.
5 J. Huang, B. Xu, C. Yuan, H. Chen, J. Sun, L. Sun and H. Ågren, *ACS Appl. Mater. Interfaces*, 2014, **6**(21), 18808.
6 F. Liu, J. Zhu, J. Wei, Y. Li, L. Hu, Y. Huang, O. Takuya, Q. Shen, T. Toyoda, B. Zhang, J. Yao and S. Dai, *J. Phys. Chem. C*, 2014, **118**(1), 214.
7 J. L. Shan, H. D. Zeng, Z. He, X. Ji, X. Ai and H. Yang, *Talanta*, 2006, **69**, 1–126.
8 G. W. Walker, V. C. Sundar, C. M. Rudzinski, A. W. Wun, M. G. Bawendi and D. G. Nocera, *Appl. Phys. Lett.*, 2003, **83**, 3555.
9 R. Dunpall, A. A. Nejo, V. S. R. Pullabhotla, A. R. Opoku, N. Revaprasadu and A. Shonhai, *IUBMB Life*, 2012, **64**(12), 995.
10 A. P. Alivisatos, W. W. Gu and C. Larabell, *Annu. Rev. Biomed. Eng.*, 2006, **7**, 55.
11 A. M. Hegazy and M. A. Abd El-Hameed, *NRIAG J. Astron. Geophys.*, 2014, **3**, 82.
12 H. Fan, P. Ju and S. Ai, *Sens. Actuators, B*, 2010, **149**(1), 98.
13 G. Oberdörster, Z. Sharp, V. Autodorei, A. Elder, R. Gelein, W. Kryeyling and C. Cox, *Inhalation Toxicol.*, 2004, **16**, 437.
14 C. B. Murray, D. J. Norris and M. G. Bawendi, *J. Am. Chem. Soc.*, 1993, **115**(19), 8706.
15 D. J. Norris, A. L. Efros, M. Rosen and M. G. Bawendi, *Phys. Rev. B: Condens. Matter Mater. Phys.*, 1996, **53**, 16347.
16 M. A. Marcus, L. E. Brus, C. Murray, M. G. Bawendi, A. Prasad and A. P. Alivisatos, *Nanostruct. Mater.*, 1992, **1**, 323.
17 X. Peng, L. Manna, W. Yang, J. Wickham, E. Scher, A. Kadavanich and A. P. Alivisatos, *Nature*, 2000, **404**, 59.
18 L. Li, J. Hu, W. Yang and A. A. Alivisatos, *Nano Lett.*, 2001, **1**(7), 349.
19 D. L. Klein, R. Roth, A. K. L. Lim, A. P. Alivisatos and P. L. McEuen, *Nature*, 1997, **389**, 699.
20 Z. A. Peng and X. Peng, *J. Am. Chem. Soc.*, 2001, **123**(1), 183.
21 Z. A. Peng and X. Peng, *J. Am. Chem. Soc.*, 2002, **124**, 3343.
22 L. Qu, Z. A. Peng and X. Peng, *Nano Lett.*, 2001, **1**, 333.
23 S. Mlowe, V. S. R. Pullabhotla, E. Mubofu, F. Ngassapa and N. Revaprasadu, *Int. Nano Lett.*, 2014, **4**, 106.
24 A. Qudhia and P. Bichpuria, *Bull. Mater. Sci.*, 2014, **37**(1), 15.
25 N. N. Dlamini, V. S. R. Rajasekhar and N. Revaprasadu, *Mater. Lett.*, 2011, **65**(9), 1280.
26 B. Susnata, S. B. Singh and S. K. Ray, *J. Solid State Chem.*, 2012, **189**, 75.
27 S. Sapra, L. A. L. Rogach and J. Feldman, *J. Mater. Chem.*, 2006, **16**, 3391.
28 B. Gao, C. Shen, S. Yuan, X. Yang and G. Chen, *J. Chin. Ceram. Soc.*, 2014, **1**(1), 1.
29 R. D. O'Brien, *Fats and oil-formulating and processing for applications*, CRC Press, Boca Raton, FL, 2nd edn, 2004.
30 D. S. Ogunyi, *Bioresour. Technol.*, 2006, **97**, 1086.
31 K. S. Liu, *J. Am. Oil Chem. Soc.*, 1994, **71**, 1179.
32 N. Weber, K. Vosmann, E. Fehling, K. D. Mukherjee and D. Bergenthal, *J. Am. Oil Chem. Soc.*, 1995, **72**(3), 361.
33 W. W. Yu, L. H. Qu, W. Guo and X. G. Peng, *Chem. Mater.*, 2003, **15**, 2854.
34 C. de Mello Donega and R. Koole, *J. Phys. Chem. C*, 2009, **113**(16), 6511.
35 J. Jasieniak, L. Smith, J. Embden and P. Mulvaney, *J. Phys. Chem. C*, 2009, **113**, 19468.
36 L. E. Brus, *J. Phys. Chem.*, 1986, **90**(12), 2555.
37 T. Kippeny, L. A. Swafford and S. J. Rosenthal, *J. Chem. Educ.*, 2002, **79**, 1094.

 This journal is © The Royal Society of Chemistry and the Centre National de la Recherche Scientifique 2015

38 V. I. Klimov, *Los Alamos Sci.*, 2003, **28**, 214.
39 Y. Y. Bacherikov, M. O. Davydenko, A. M. Dmytruck, L. M. Dmytruck, P. M. Lytvyn, V. Prokopenko and V. R. Romanyuk, *Optoelectronics*, 2006, **9**(2), 75.
40 J. M. Nedeljkovic, R. C. Patel, P. Kaufman, C. Joyce and P. O'Leary, *J. Chem. Educ.*, 1993, **70**, 342.
41 M. Green and P. O'Brien, *Chem. Commun.*, 1999, 2235.
42 A. L. Patterson, *Phys. Rev.*, 1939, **56**, 978.
43 B. Vaisman, A. Shikanov and A. J. Domb, *J. Am. Oil Chem. Soc.*, 2008, **85**, 169.
44 O. S. Oluwafemi and N. Revaprasadu, *New J. Chem.*, 2008, **10**, 1432.

Published on 21 July 2015. Downloaded by University of Zululand on 06/10/2015 13:12:41.